Available online at www.sciencedirect.com

ScienceDirect

journal homepage: http://www.elsevier.com/locate/medici

Original Research Article

Accumulation and biological effects of cobalt ferrite nanoparticles in human pancreatic and ovarian cancer cells

Vita Pašukonienė [a,*], Agata Mlynska [a], Simona Steponkienė [b], Vilius Poderys [b], Marija Matulionytė [b,c], Vitalijus Karabanovas [b], Urtė Statkutė [b], Rasa Purvinienė [a], Jan Aleksander Kraśko [a], Arūnas Jagminas [d], Marija Kurtinaitienė [d], Marius Strioga [a], Ričardas Rotomskis [b,c]

[a] Laboratory of Immunology, National Cancer Institute, Vilnius, Lithuania
[b] Biomedical Physics Laboratory, National Cancer Institute, Vilnius, Lithuania
[c] Biophotonics Group of Laser Research Centre, Faculty of Physics, Vilnius University, Vilnius, Lithuania
[d] Laboratory of Nanostructures, State Research Institute Centre for Physical Sciences and Technology, Vilnius, Lithuania

ARTICLE INFO

Article history:
Received 30 April 2014
Accepted 25 September 2014
Available online 6 October 2014

Keywords:
Superparamagnetic cobalt ferrite nanoparticles
Cytotoxicity
Pancreatic cancer
Ovarian cancer
Cancer stem-like cells

ABSTRACT

Background and objective: Superparamagnetic iron oxide nanoparticles (SPIONs) emerge as a promising tool for early cancer diagnostics and targeted therapy. However, both toxicity and biological activity of SPIONs should be evaluated in detail. The aim of this study was to synthesize superparamagnetic cobalt ferrite nanoparticles (Co-SPIONs), and to investigate their uptake, toxicity and effects on cancer stem-like properties in human pancreatic cancer cell line MiaPaCa2 and human ovarian cancer cell line A2780.

Materials and methods: Co-SPIONs were produced by Massart's co-precipitation method. The cells were treated with Co-SPIONs at three different concentrations (0.095, 0.48, and 0.95 μg/mL) for 24 and 48 h. Cell viability and proliferation were analyzed after treatment. The stem-like properties of cells were assessed by investigating the cell clonogenicity and expression of cancer stem cell-associated markers, including CD24/ESA in A2780 cell line and CD44/ALDH1 in MiaPaCa2 cell line. Magnetically activated cell sorting was used for the separation of magnetically labeled and unlabeled cells.

Results: Both cancer cell lines accumulated Co-SPIONs, however differences in response to nanoparticles were observed between MiaPaCa2 and A2780 cell. In particular, A2780 cells were more sensitive to exposition to Co-SPIONs than MiaPaCa2 cells, indicating that a safe concentration of nanoparticles must be estimated individually for a particular cell type. Higher doses of Co-SPIONs decreased both the clonogenicity and ESA marker expression in A2780 cells.

* *Corresponding author at:* Laboratory of Immunology, National Cancer Institute, Santariškių 1, 08660 Vilnius, Lithuania.
E-mail address: vita.pasukoniene@nvi.lt (V. Pašukonienė).

Peer review under the responsibility of the Lithuanian University of Health Sciences.

Production and hosting by Elsevier

http://dx.doi.org/10.1016/j.medici.2014.09.009

Conclusions: Co-SPIONs are not cytotoxic to cancer cells, at least when used at a concentration of up to 0.95 μg/mL. Co-SPIONs have a dose-dependent effect on the clonogenic potential and ESA marker expression in A2780 cells. Magnetic detection of low concentrations of Co-SPIONS in cancer cells is a promising tool for further applications of these nanoparticles in cancer diagnosis and treatment; however, extensive research in this field is needed.

1. Introduction

Nanotechnologies have a great potential for various biomedical applications, including cancer diagnostics and treatment [1–4]. Superparamagnetic iron oxide nanoparticles (SPIONs) were the first nanoscale materials approved for clinical use as contrast agents for magnetic resonance imaging (MRI) of liver [5] and lymph nodes [6]. SPIONs also allow a targeted delivery of drugs, proteins and genes [7], cell bioimaging [8], and induction of cell death by the hyperthermia effect [9].

Different types of SPIONs, varying in their composition and/or surface coating, can be synthesized, depending on the requirements for their application [10–12]. Considering current limitations in the field in terms of SPION application in routine clinical practice, we aimed to synthesize and investigate a specific type of SPIONs – superparamagnetic cobalt ferrite nanoparticles (Co-SPIONs) – that are attractive candidates for magnetic resonance imaging (MRI), magnetic field-assisted drug delivery and magnetothermal therapy of cancer and other diseases. Owing to a mixed spinel structure [13], the properties of Co-SPIONs depend not only on their size and shape, but also on the cobalt content [14,15]. Due to high saturation magnetization, low coercivity, excellent chemical and thermal stability [16], Co-SPIONs possess a great potential for a wide application both in biomedical research and clinical practice.

However, there are no data about biological activity of Co-SPIONs, including their cellular uptake, toxicity, effects on cell proliferation, phenotype and functional activity. Therefore, these aspects remain a subject of particular interest.

In this study, we aimed to investigate the accumulation and biological effects of Co-SPIONs, originally synthesized by our group. Two well-characterized cancer cell lines (human pancreatic cancer cell line MiaPaCa2 and human ovarian cancer cell line A2780) served as biological models in our in vitro experiments. Both cell lines are poorly differentiated, highly tumorigenic and heterogeneous, with certain phenotypic subsets attributable to cancer stem cell-like properties [17–19]. We sought to evaluate the potential of using Co-SPIONs in clinical applications, since pancreatic and ovarian cancers are among the most aggressive and intractable oncological diseases, which could benefit from improved means of diagnosis and treatment [20,21].

2. Materials and methods

2.1. Synthesis and characterization of Co-SPIONs

Co-SPIONs were synthesized in the thermostated glass reactor by Massart's co-precipitation method [22] from the alkaline solutions of Co(II) and Fe(III) metal salts at 70 °C for 5 h. All reagents used for Co-SPION synthesis were at least of analytical grade, thus they were not additionally purified, except for NaOH, which was purified by preparation of a saturated solution resulting in the crystallization of other sodium salts. $CoCl_2$, $Fe_2(SO_4)_3$ and citric acid were purchased from Aldrich Chemicals Inc. For preparation of the working solutions 0.12 mol/L $CoCl_2$, 0.06 mol/L $Fe_2(SO_4)_3$, 5.0 mol/L NaOH, and 0.3 mol/L citric acid solutions were prepared and deoxygenated with argon before mixing. Ultrapure water was used throughout all procedures. Molar ratio of cobalt(II) and iron(III) salts in the reactor was 1:1.2 at their total concentration of 40 mmol/L. pH of solutions was maintained at 11.5. The required amount of 5.0 mol/L NaOH solution was predetermined in a blank experiment. In the subsequent experiments, the estimated amount of NaOH was added to the reactor, containing all other components, in several seconds under vigorous stirring. The synthesis in the thermostated reactor was conducted under a continuous argon gas bubbling. Crude products were centrifuged at 2800 × *g* for 5 min and rinsed several times. The supernatants obtained from the last three centrifugations were mixed, neutralized by the addition of citric acid solution up to pH 6.0, and used as a stable ferrofluid within the following week. The composition of the synthesized products was investigated by energy dispersive X-ray spectroscopy and nanoparticle dissolution in HCl (1:1) solution by inductively plasma coupled optical emission spectrometry, using an OPTIMA 7000DV analyzer (Perkin Elmer, USA).

The morphology of Co-SPIONs was investigated with an atomic force microscope Veeco-dilnnova (Veeco Inc., USA), using a tapping mode. A small amount (40 μL) of Co-SPION solution was dropped on a freshly cleaved mica surface, spinning at 50 × *g*. Zeta potential of the particles was measured using a Brookhaven ZetaPALS zeta potential analyzer (Brookhaven Instruments, USA).

Magnetic measurements of Co-SPIONs were carried out on a vibrating sample magnetometer. A gauss-/teslameter FH-54 (Magnet Physik, Germany) was applied to measure the

strength of the magnetic field between the poles of the laboratory magnet SM 330-AR-22 (Delta Elektronika, Netherlands). A lock-in amplifier SR510 (Stanford Research Systems, USA) was used to measure the signal from the sense coils.

2.2. Cell culture

Human pancreatic cancer cell line MiaPaCa2 and human ovarian cancer cell line A2780 were purchased from the European Collection of Cell Cultures (UK). MiaPaCa2 cells were cultured in Dulbecco's Modified Eagle Medium. A2780 cells were cultured in Roswell Park Memorial Institute 1640 medium. Both growth media were supplemented with 10% fetal bovine serum, 100 U/mL penicillin and 100 mg/mL streptomycin. All media and cell culture supplements were purchased from Biochrom AG (Germany). Cells were cultured in a humified 37 °C, 5% CO_2 atmosphere and subcultured twice a week.

2.3. Cell treatment with Co-SPIONs

Cells in a log phase were plated in surface-treated cell culture dishes at an appropriate density (3×10^4 cells/cm^2 for MiaPaCa2 and 4×10^4 cells/cm^2 for A2780) and cultured in a CO_2 incubator for 24 h. Afterwards, Co-SPIONs were added to cell growth medium.

For a Co-SPION accumulation assay, cells were plated in 35 mm Petri dish (containing 2 mL of growth medium), treated with Co-SPIONs (at a concentration of 0.48 μg/mL), and incubated for 24 h. Untreated cells were used as controls. After treatment with Co-SPIONs the cells were routinely rinsed 3 times with PBS and fixed with paraformaldehyde (4%) for 15 min. Prussian Blue Cell Staining Reagent Pack (BioPAL) was used to visualize the iron content within the cells. Equal amounts of both reagents A (hydrochloric acid) and B (potassium ferrocyanide) were combined, added to fixed cells and left for 15 min. Staining solution was then aspirated; the cells were rinsed 3 times with PBS and imaged using a brightfield mode of a Nikon Eclipse TE2000 EZ-C1 microscope (Japan).

For cell proliferation and viability analysis, cells were plated in 6-well plates, treated with Co-SPIONs (at concentrations of 0.095, 0.48, and 0.95 μg/mL) in 2 mL of growth medium per well and incubated for 24 and 48 h. Untreated cells were used as controls. After treatment, the growth medium was removed by aspiration and adherent cells were detached from a culture surface by trypsinization. Accustain Kit (Digital Bio, Korea) was used to determine cell viability. The cells were stained with AccuStain Solution T (propidium iodide + lysis solution) for the total cell staining and with AccuStain Solution N (fluorescent dye + PBS) for non-viable cell staining. Cell viability was calculated with an automated cell counter ADAM (NanoEnTek, Korea). For clonogenicity (colony-forming) assay, cells were harvested after 48 h of incubation with Co-SPIONs, counted and plated at an appropriate density (300 cells per well for MiaPaCa2 line, 200 cells per well for A2780 line) in 6-well plates. After 6–10 days, cell colonies were fixed with ethanol, stained with crystal violet dye, and counted with an automated colony counter ColonyDoc-It (UVP BioImaging Systems, USA). Colony was defined as a cluster of a minimum of 50 cells. Colony-forming efficiency (CFE) was calculated as a percentage of colonies per total cells plated.

2.4. Flow cytometry

The size and granularity of the Co-SPION-treated cells were analyzed with a BD LSR II flow cytometer (BD Biosciences, USA). The expression of stemness-associated proteins was determined by labeling of up to 10^6 cells with 5 μL of mouse monoclonal anti-human antibodies. For A2780 cells we used anti-CD24 antibody conjugated to fluorescein isothiocyanate (FITC) (1:20 dilution, BD Biosciences, USA) and anti-epithelial specific antigen (ESA) antibody conjugated to phycoerythrin (PE) (1:75 dilution, eBiosciences, USA). For MiaPaCa2 cells we used anti-CD44 antibody conjugated to PE (1:20 dilution, BD Biosciences, USA) and ALDEFLUOR Kit (STEMCELL Technologies, Canada) for aldehyde dehydrogenase-1 (ALDH1) activity. For each sample, 10,000 cells were acquired using a BD FACSDiva software (BD Biosciences, USA) and analyzed with a FlowJo software (Tree Star, USA). Dead cells were gated out using 7-aminoactinomycin D (BD Biosciences, USA) staining.

2.5. Magnetic-activated cell sorting

Magnetically activated cell sorting (MACS) was used to separate magnetically labeled and unlabeled cells after 48-h incubation with Co-SPIONs. The principle of MACS is presented in Fig. 1. A single-cell suspension of the treated cells was passed through an LS Column, placed in a MidiMACS Separator (Miltenyi Biotec, Germany). Co-SPION-unlabeled fraction passed through the column, whereas Co-SPION-labeled fraction remained in the column. This fraction was collected by removing the LS Column from magnetic field and eluting the attached cells with PBS. Both fractions were examined under both microscope and cell counter for the presence of cells.

2.6. Statistical analysis

Triplicate measurements of each sample were performed in three independent experiments. Statistical differences between the groups were analyzed by Student's *t* test. A value of $P < 0.05$ was considered significant.

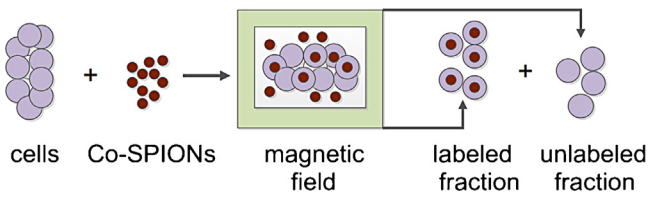

Fig. 1 – The principle of MACS cell separation. Cells are incubated with magnetic particles (e.g. Co-SPIONs) and passed through magnetic field. The flow-through is collected as magnetically unlabeled fraction. Cells retained in magnetic field are flushed out as magnetically labeled fraction.

3. Results

3.1. Size, composition and magnetic properties of Co-SPIONs

Atomic force microscopy images (Fig. 2A) revealed that Co-SPIONs synthesized for this study were almost spherical with particle sizes ranging from 1 to 15 nm. The majority of nanoparticles were between 3 and 5 nm in size (Fig. 2B). However some large (up to 300 nm in diameter) aggregates of Co-SPIONs were also present on mica surface. Zeta potential of nanoparticles was −26 mV. Chemical analysis indicated that the structural composition of particular Co-SPIONs was $Co_{0.84}Fe_{2.16}O_4$. The M–B curve of cobalt ferrite nanoparticles shows its superparamagnetic nature with low coercivity (Fig. 2C).

3.2. Cellular accumulation of Co-SPIONs

Cellular accumulation of nanoparticles was visualized using an iron labeling technique and a bright field mode of a laser scanning confocal microscope (Fig. 3). We found that a 24-h incubation of cells with 0.48 μg/mL of Co-SPIONs, resulted in the intracellular accumulation and perinuclear localization of nanoparticles in both cell lines

3.3. Cell viability after treatment with Co-SPIONs

Measurement of cell viability showed that 0.095, 0.48, and 0.95 μg/mL concentrations of Co-SPIONs had little effect on both cell lines (Fig. 4). No significant differences in viability between control and treated groups were observed after 24 and 48 h of incubation with nanoparticles in MiaPaCa2 cells. In A2780 cells, there was a slight decrease in the viability of cells treated with 0.095–0.95 μg/mL concentration of Co-SPIONs for 48 h (87%–90%) in comparison to control (87%–90% versus 97%, respectively).

3.4. Cell proliferation after treatment with Co-SPIONs

Cell proliferation in response to Co-SPIONs differed between the two cell lines (Fig. 5). We did not observe any significant differences in MiaPaCa2 cell line, independently of the duration of treatment. For A2780 cells, the antiproliferative effect of Co-SPIONs was not observed with 24-h incubation; however, after 48 h of incubation, a 0.48 μg/mL concentration of Co-SPIONs was sufficient for a significant inhibition of cell proliferation. The number of proliferating cells treated with 0.48 and 0.95 μg/mL of Co-SPIONs was 22.0×10^5 and 18.4×10^5, respectively, and it was nearly two-fold lower in comparison with control (36.9×10^5 viable cells).

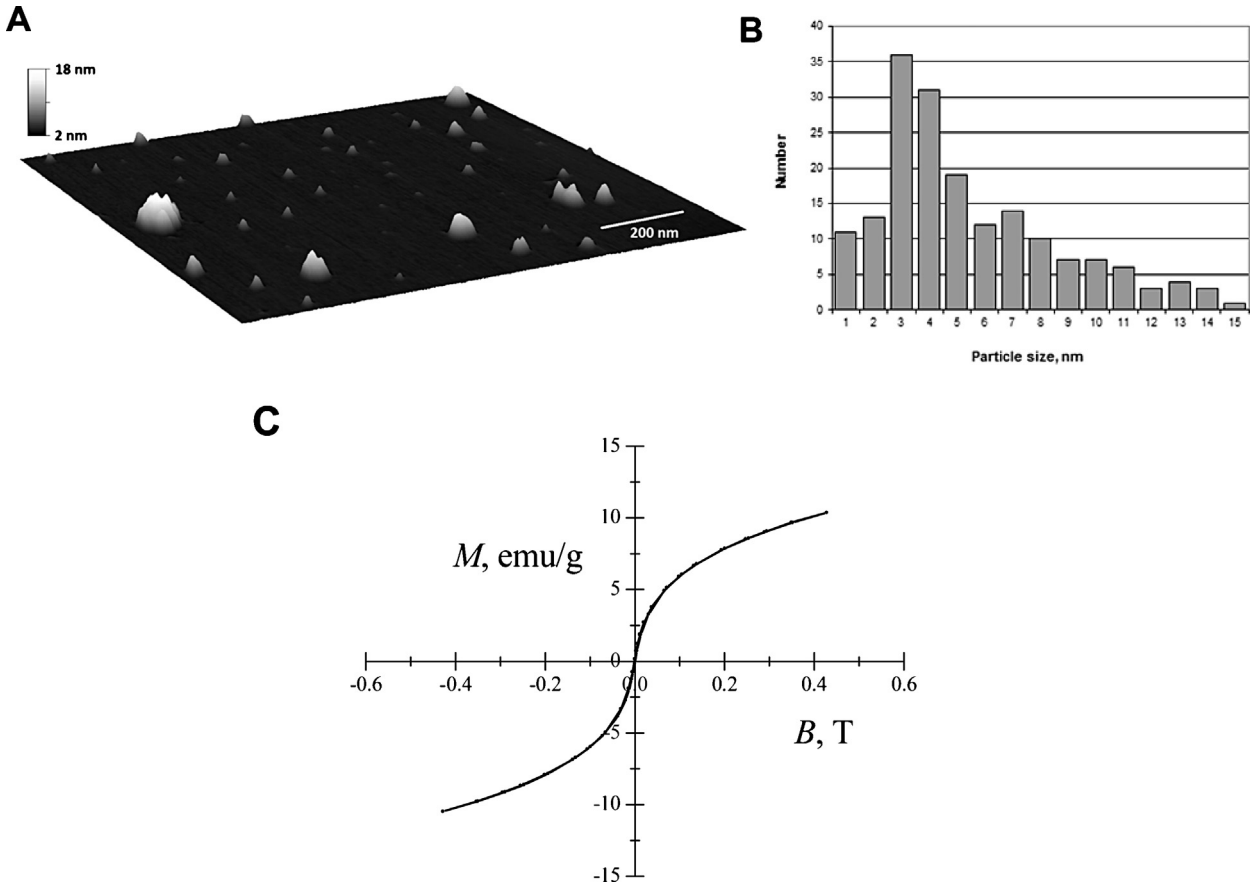

Fig. 2 – Atomic force microscopy topographic 3D image (A) particle size distribution (B) and magnetization curve (C) of Co-SPIONs synthesized by citric acid-assisted co-precipitation route from Co(II) and Fe(III) precursors at their 1:1.2 molar ratio and 40 mmol/L total concentration in argon atmosphere at 70 °C for 5 h; pH 11.5.

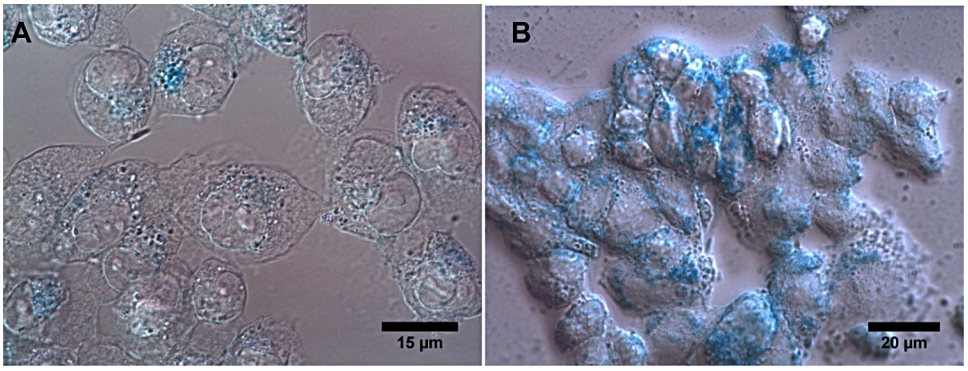

Fig. 3 – Images of ×60 magnification of cells stained with Prussian blue. (A) MiaPaCa2 cells treated with 0.48 μg/mL of Co-SPION, (B) A2780 cells treated with 0.48 μg/mL of Co-SPIONs. Blue spots show magnetic nanoparticles. (For interpretation of the references to color in this figure legend, the reader is referred to the web version of this article.)

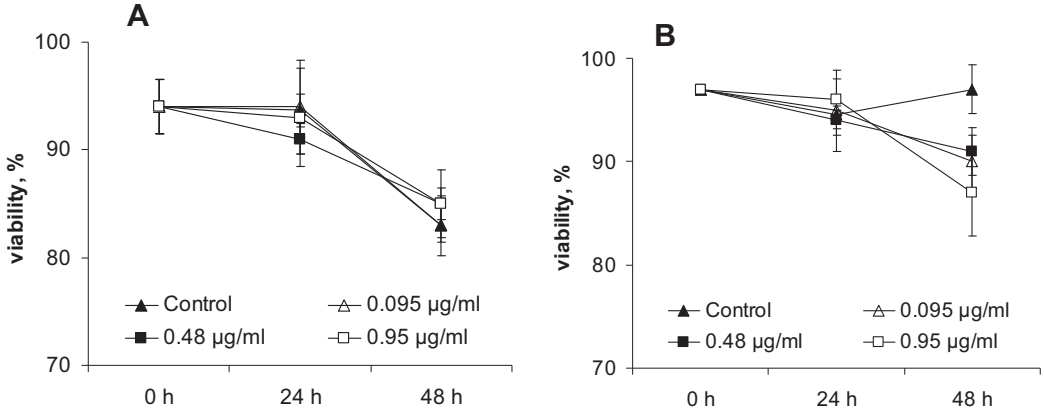

Fig. 4 – Effect of Co-SPION concentration and time of incubation on cell viability in MiaPaCa2 (A) and A2780 (B) cell lines. The percentage of viable cells was evaluated prior to treatment and after 24 and 48 h of incubation. Results of triplicate measurements are shown (mean ± standard deviation).

3.5. *The effect of Co-SPIONs on clonogenicity of cancer cells*

We observed differences in colony formation capacity between MiaPaCa2 and A2780 cell lines after treatment with different concentrations of Co-SPIONs (Fig. 6). Clonogenicity of MiaPaCa2 cells was independent of Co-SPIONs dose. CFE remained stable (28.4%–30.4%) for both untreated and treated cells. In contrast, clonogenicity of A2780 cells was dependent on Co-SPION dose. CFE gradually decreased from 54% in the control group to 37% following treatment with 0.95 μg/mL of Co-SPIONs.

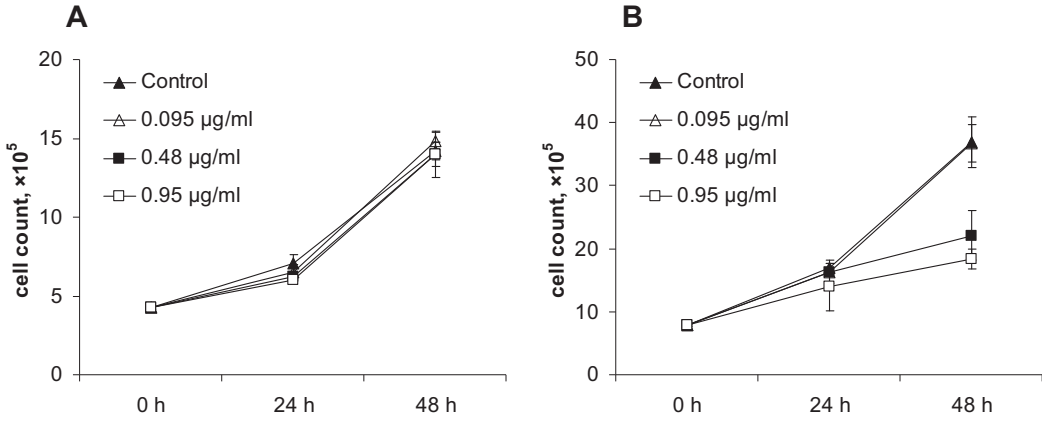

Fig. 5 – Effect of Co-SPION concentration and time of incubation on cell proliferation in MiaPaCa2 (A) and A2780 (B) cell lines. The percentage of viable cells was evaluated prior to treatment and after 24 and 48 h of incubation. Results of triplicate measurements are shown (mean ± standard deviation).

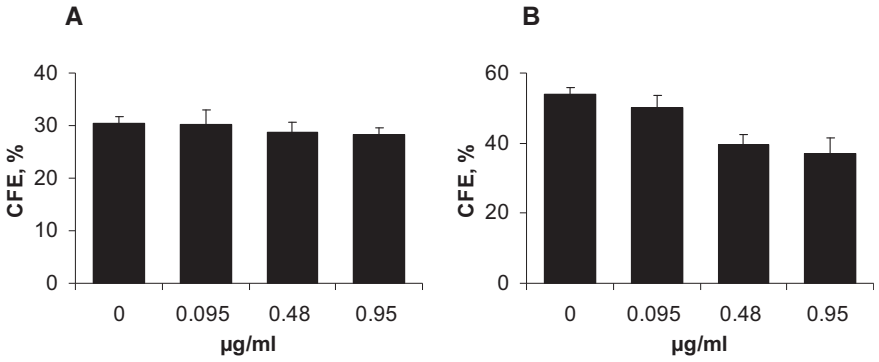

Fig. 6 – Co-SPIONs effect on clonogenicity in MiaPaCa2 (A) and A2780 (B) cell lines. Columns represent untreated cells (0) and groups treated with different concentrations of Co-SPIONs (0.095, 0.48, and 0.95 μg/mL). Colony-forming efficiency was calculated 6–10 days post Co-SPIONs treatment. Results of triplicate measurements are shown (mean ± standard deviation).

3.6. *Cell phenotype*

The expression of selected protein biomarkers was assessed after 48-h incubation with Co-SPIONs. Results are summarized in Table. In MiaPaCa2 cell line, almost all control cells were positive for CD44 and ALDH1 and no significant changes in cell phenotype were observed after treatment with Co-SPIONs. A2780 cells were negative for CD24 marker, whereas 9.3% of the cells were positive for ESA marker. Co-SPIONs did not have any effect on CD24 marker expression. However, we observed significant changes in ESA expression. ESA-positive cell subset tends to decrease with higher doses of Co-SPIONs used for treatment.

Table – Percentage changes of expression in stemness-associated biomarkers in cells treated with different concentrations of Co-SPIONs[a]

	A2780		MiaPaCa2	
	CD24	ESA	CD44	ALDH1
Control	0.9	9.3	98.2	95.4
0.095 μg/mL	0.7	8.2	97.8	96.7
0.48 μg/mL	0.9	8.1	98.5	96.4
0.95 μg/mL	0.8	7.2	99.0	96.2

[a] Percentage of marker-positive population out of 10,000 cells is shown.

3.7. *Magnetic separation of Co-SPION-labeled and -unlabeled cells*

After microscopy and counting of magnetically sorted cells, we observed differences in Co-SPION accumulation between MiaPaCa2 and A2780 cell lines (Fig. 7). MiaPaCa2 cells treated with 0.095, 0.48, and 0.95 μg/mL of Co-SPIONs were all separated into both labeled and unlabeled fractions. Unlike MiaPaca2 cells, A2780 cells treated with 0.48 and 0.95 μg/mL concentrations of Co-SPIONs were all magnetically labeled. Only A2780 cells treated with 0.095 μg/mL concentrations were sorted into labeled and unlabeled fractions.

4. Discussion

In this study, we aimed to evaluate the biological effects of previously synthesized Co-SPIONs on human pancreatic

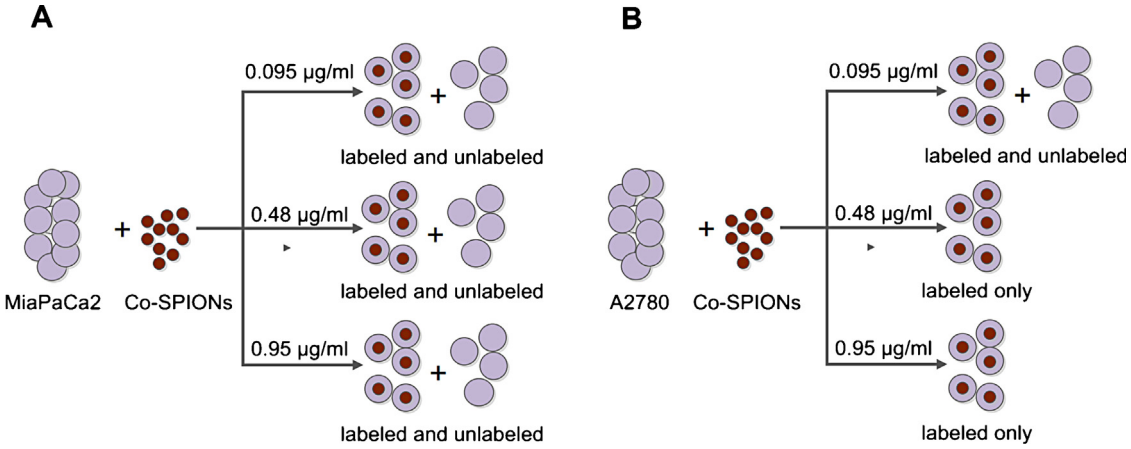

Fig. 7 – Labeling of MiaPaCa2 (A) and A2780 (B) cell lines with different concentrations of Co-SPIONs (0.095, 0.48 and 0.95 μg/mL) after MACS cell sorting.

cancer cell line MiaPaCa2 and human ovarian cancer cell line A2780. We investigated the uptake and toxicity of Co-SPIONs, as well as their influence on clonogenicity and expression of biomarkers, attributable to the cancer stem-like phenotype [23]. Our results show that although Co-SPIONs accumulated in both cell lines, some differences were observed in cell response to nanoparticles.

Co-SPIONs at concentrations of 0.095–0.95 μg/mL had no effect on MiaPaCa2 cell proliferation. However, we observed a decrease in cell number of A2780 cells after treatment with the same concentrations of nanoparticles. Interestingly, 0.48 μg/mL concentration of Co-SPIONs was the threshold dose for both inhibition of cell proliferation and total magnetic labeling in A2780 cells. In contrast, MiaPaCa2 cells were less susceptible to Co-SPIONs, since both magnetically labeled and unlabeled subsets were identified even after treatment with the greatest concentration of SPIONs. The data imply that Co-SPION doses capable of total labeling of cells may also exhibit an antiproliferative activity in ovarian cancer cell line A2780. Although these results are not sufficient for revealing the mechanisms of such presumptive dependence, they still allow us to speculate that Co-SPIONs are capable of reducing cancer cell proliferation if delivered properly.

Cell viability analysis indicates that Co-SPIONs at concentrations of 0.095–0.95 μg/mL are nontoxic for both cell lines. The results support the data from other studies, where low or no cytotoxicity associated with SPIONs was generally found until high exposure levels [24–26]. With regard to the underlying mechanisms of high dose SPION-mediated cytotoxicity, there are data that SPIONs may disturb cellular iron balance, modify various signaling pathways, induce DNA damage, oxidative stress, mechanical alterations of cytoskeleton or changes in gene expression [12].

Clonogenicity is a reliable parameter to determine the capability of the cells to duplicate, multiply and survive during the exposition to chemical or radiation challenges [27]. Both cell lines differed in their clonogenic potential after treatment with Co-ferrite SPIONs. Colony forming capacity of MiaPaCa2 cells remained stable, regardless of Co-SPION concentration. Similarly, no changes in the expression of CD44 and ALDH1 were observed. Since results of MiaPaCa2 clonogenicity assay provide a reliable supplement for cell accumulation and proliferation data, we suggest that this cell line is not sensitive to Co-SPIONs.

While investigating the Co-SPIONs influence on A2780 cell line clonogenicity and ESA expression, we observed a dose-dependent relationship of a cell response to treatment. The higher was the dose of Co-SPIONs, the lower the clonogenicity and ESA marker expression was observed in A2780 cells. A decrease in the expression of ESA marker, which plays a role in promoting metastasis and is typical to cancer stem cells [28], implies that Co-SPIONs may have a significant effect on cell phenotype without the influence on cell viability. Assuming that both higher clonogenicity and ESA expression are representative of putative cancer stem cells, it is possible that, at appropriate doses, Co-SPIONs may preferentially target these cells and inhibit their stem-like properties. It has been demonstrated that SPIONs are able to inhibit colony formation of bone marrow-derived mesenchymal stem/stromal cells [29]. In contrast to these findings, another group did not observe any significant effect of SPIONs on the ''stemness'' of MSCs [30]. It should be noted that SPIONs of different diameter were used in these independent studies. Taking into account that properties of nanoparticles may change with their size these results should be evaluated prudently.

Our study provided a comprehensive approach to Co-SPIONs effect on human pancreatic and ovarian cancer lines in vitro, covering aspects of nanoparticle uptake and toxicity as well as their influence on stemness-associated properties. SPIONs emerge as an invaluable future instrument for new multifunctional theragnostic nanoplatforms clinical oncological practice. Magnetic nanoparticles are promising tool for diagnosis of cancer using magnetic resonance and/or optical imaging, and treatment through the combination of chemical, photothermal and magnetothermal therapy. Future studies should explore the exact mechanisms of Co-SPION uptake, efflux and accumulation in cells in more detail. Moreover, improvements in nanoparticle design, allowing specific targeting of tumor tissue, may greatly enhance the application of nanotechnologies in clinical practice.

5. Conclusions

This study provides some initial evidence that Co-SPIONs are noncytotoxic and may serve as a powerful tool for tumor detection and magnetic field-assisted targeted chemotherapy or magnetothermal therapy. Our findings demonstrate that human pancreatic cancer cell line MiaPaCa2 and human ovarian cancer cell line A2780 differ in their ability to accumulate Co-SPIONs, therefore a safe concentration of nanoparticles must be estimated individually. Co-SPIONs have a dose-dependent effect on A2780 cell clonogenicity and ESA marker expression. Further extensive research in this field is promising and reasonable.

Conflict of interest

The authors state no conflicts of interest.

Acknowledgments

This study was supported by the Research Council of Lithuania Grant No LIG-15/2010 and Grant No MIP-088/2011.

REFERENCES

[1] Davis ME, Chen ZG, Shin DM. Nanoparticle therapeutics: an emerging treatment modality for cancer. Nat Rev Drug Discov 2008;7(9):771–82.
[2] De Jong WH, Borm PJ. Drug delivery and nanoparticles: applications and hazards. Int J Nanomed 2008;3(2):133–49.
[3] Wang MD, Shin DM, Simons JW, Nie S. Nanotechnology for targeted cancer therapy. Expert Rev Anticancer Ther 2007;7(6):833–7.

[4] Clausell-Tormos J, Heeschen C. Pancreatic cancer stem cells as new targets for diagnostics and therapy. Else Kroner Fresen Symp 2011;2:116–34.
[5] Stark DD, Weissleder R, Elizondo G, Hahn PF, Saini S, Todd LE, et al. Superparamagnetic iron oxide: clinical application as a contrast agent for MR imaging of the liver. Radiology 1988;168(2):297–301.
[6] Weissleder R, Elizondo G, Wittenberg J, Lee AS, Josephson L, Brady TJ. Ultrasmall superparamagnetic iron oxide: an intravenous contrast agent for assessing lymph nodes with MR imaging. Radiology 1990;175(2):494–8.
[7] Gupta AK, Gupta M. Synthesis and surface engineering of iron oxide nanoparticles for biomedical applications. Biomaterials 2005;26(18):3995–4021.
[8] Mou Y, Hou Y, Chen B, Hua Z, Zhang Y, Xie H, et al. In vivo migration of dendritic cells labeled with synthetic superparamagnetic iron oxide. Int J Nanomed 2011;6:2633–40.
[9] Silva AC, Oliveira TR, Mamani JB, Malheiros SMF, Malavolta L, Pavon LF, et al. Application of hyperthermia induced by superparamagnetic iron oxide nanoparticles in glioma treatment. Int J Nanomed 2011;6:591–603.
[10] Berry CC, Wells S, Charles S, Aitchison G, Curtis ASG. Cell response to dextran-derivatised iron oxide nanoparticles post internalisation. Biomaterials 2004; 25(23):5405–13.
[11] Mahmoudi M, Simchi A, Milani AS, Stroeve P. Cell toxicity of superparamagnetic iron oxide nanoparticles. J Colloid Interface Sci 2009;336(2):510–8.
[12] Singh N, Jenkins GJ, Asadi R, Doak SH. Potential toxicity of superparamagnetic iron oxide nanoparticles (SPION). Nano Rev 2010;1.
[13] Nakagomi F, da Silva SW, Garg VK, Oliveira AC, Morais PC, Junior AF, et al. The influence of cobalt population on the structural properties of $CoxFe_3$-xO_4. J Appl Phys 2007; 101(9).
[14] Liu C, Zou BS, Rondinone AJ, Zhang J. Chemical control of superparamagnetic properties of magnesium and cobalt spinel ferrite nanoparticles through atomic level magnetic couplings. J Am Chem Soc 2000;122(26):6263–7.
[15] Rajendran M, Pullar RC, Bhattacharya AK, Das D, Chintalapudi SN, Majumdar CK. Magnetic properties of nanocrystalline $CoFe_2O_4$ powders prepared at room temperature: variation with crystallite size. J Magn Magn Mater 2001;232(1–2):71–83.
[16] Naseri MG, Saion EB, Ahangar HA, Shaari AH, Hashim M. Simple synthesis and characterization of cobalt ferrite nanoparticles by a thermal treatment method. J Nanomater 2010. http://dx.doi.org/10.1155/2010/907686. Article ID: 907686, 8 pages.
[17] Deer EL, Gonzalez-Hernandez J, Coursen JD, Shea JE, Ngatia J, Scaife CL, et al. Phenotype and genotype of pancreatic cancer cell lines. Pancreas 2010;39(4):425–35.
[18] Bao B, Azmi A, Aboukameel A, Ahmad A, Bolling-Fischer A, Sethi S, et al. Pancreatic cancer stem-like cells display aggressive behavior mediated via activation of FoxQ1. J Biol Chem 2014;289(21):14520–33.
[19] Baba T, Convery PA, Matsumura N, Whitaker RS, Kondoh E, Perry T, et al. Epigenetic regulation of CD133 and tumorigenicity of CD133+ ovarian cancer cells. Oncogene 2009;28(2):209–18.
[20] Philip PA, Mooney M, Jaffe D, Eckhardt G, Moore M, Meropol N, et al. Consensus report of the national cancer institute clinical trials planning meeting on pancreas cancer treatment. J Clin Oncol 2009;27(33):5660–9.
[21] Kurzeder C, Sauer G, Deissler H. Molecular targets of ovarian carcinomas with acquired resistance to platinum/ taxane chemotherapy. Curr Cancer Drug Target 2006; 6(3):207–27.
[22] Massart R. Preparation of aqueous magnetic liquids in alkaline and acidic media. IEEE Trans Magn 1981;17(2):1247.
[23] Clevers H. The cancer stem cell: premises, promises and challenges. Nat Med 2011;17(3):313–9.
[24] Berry CC, Wells S, Charles S, Curtis ASG. Dextran and albumin derivatised iron oxide nanoparticles: influence on fibroblasts in vitro. Biomaterials 2003;24(25):4551–7.
[25] Mahmoudi M, Simchi A, Imani M, Shokrgozar MA, Milani AS, Hafeli UO, et al. A new approach for the in vitro identification of the cytotoxicity of superparamagnetic iron oxide nanoparticles. Colloids Surf B Biointerfaces 2010;75 (1):300–9.
[26] Przybytkowski E, Behrendt M, Dubois D, Maysinger D. Nanoparticles can induce changes in the intracellular metabolism of lipids without compromising cellular viability. FEBS J 2009;276(21):6204–17.
[27] Baumann M, Krause M, Hill R. Clonogens and cancer stem cells. Nat Rev Cancer 2008;8(12).
[28] van der Gun BT, Melchers LJ, Ruiters MH, de Leij LF, McLaughlin PM, Rots MG. EpCAM in carcinogenesis: the good, the bad or the ugly. Carcinogenesis 2010;31 (11):1913–21.
[29] Schafer R, Kehlbach R, Wiskirchen J, Bantleon R, Pintaske J, Brehm BR, et al. Transferrin receptor upregulation: in vitro labeling of rat mesenchymal stem cells with superparamagnetic iron oxide. Radiology 2007;244(2):514–23.
[30] Balakumaran A, Pawelczyk E, Ren J, Sworder B, Chaudhry A, Sabatino M, et al. Superparamagnetic iron oxide nanoparticles labeling of bone marrow stromal (mesenchymal) cells does not affect their ''stemness''. PLoS ONE 2010;5(7):e11462.